Joint Adaptive Modulation and Diversity Combining with Feedback Error Compensation

Seyeong Choi (seyeong.choi@qatar.tamu.edu)

Texas A&M University at Qatar

Hong-Chuan Yang (hyang@ece.uvic.ca)

University of Victoria

Mohamed-Slim Alouini (alouini@qatar.tamu.edu)

Texas A&M University at Qatar

Khalid A. Qaraqe (khalid.qaraqe@qatar.tamu.edu)

Texas A&M University at Qatar

Abstract

This report investigates the effect of feedback error on the performance of the joint adaptive modulation and diversity combining (AMDC) scheme which was previously studied with an assumption of error-free feedback channels. We also propose to utilize adaptive diversity to compensate for the performance degradation due to feedback error. We accurately quantify the performance of the joint AMDC scheme in the presence of feedback error, in terms of the average number of combined paths, the average spectral efficiency, and the average bit error rate. Selected numerical examples are presented and discussed to illustrate the effectiveness of the proposed feedback error compensation strategy with adaptive combining. It is observed that the proposed compensation strategy can offer considerable error performance improvement with little loss in processing power and spectral efficiency in comparison with the no compensation case.

CONTENTS

LIST OF TABLES

LIST OF FIGURES

I. Introduction

Because of the growing demand for a higher spectral efficiency as well as a good link reliability in wireless communications, many new technologies have been proposed over the last few decades. Among them, adaptive transmission aims to optimize the transmission rate according to the fading channel variations. It has been shown that a considerable gain in throughput can be achieved by using adaptive transmission while maintaining a certain target error rate performance and assuming an error-free feedback channel [1]–[4]. On the other hand, diversity technique refers to a method for improving the reliability of wireless fading channels by utilizing two or more communication channels with different characteristics and as such, it plays an important role in combatting fading and co-channel interference. Various classical diversity combining techniques can be found in [5]–[10].

Recently, as an attempt to obtain further improved spectral efficiency under the same error rate requirement, some joint adaptive modulation and diversity combining (AMDC) schemes were proposed and analyzed in [11]–[13]. Unlike [14], [15] which are some earlier AMDC works focusing on the channel capacity, [11]–[13] employ more sophisticated diversity combining techniques such as generalized selection combining (GSC) [16]–[19], minimum selection-GSC (MS-GSC) [20]–[22], minimum estimation and combining-GSC (MEC-GSC) [23], and output threshold-maximum ratio combining (OT-MRC) [24]. With the schemes in [11]–[13], the receiver jointly decides the proper modulation mode and diversity combiner structure based on the channel quality and the target error rate requirement. Different mode of operations have been considered based on the primary optimization criteria of the joint design. For example, the power-efficient AMDC scheme leads to a high processing power efficiency, the bandwidth-efficient AMDC scheme leads to a high bandwidth efficiency, and the bandwidth-efficient and power-greedy AMDC scheme leads to a high bandwidth efficiency as well as an improved power efficiency at the cost of a higher error rate in comparison with the bandwidth-efficient AMDC scheme.

In most of the published papers dealing with adaptive modulation, it is generally assumed for analytical tractability that the feedback channel is error-free. However, there are a number of

real-life scenarios in which this ideal assumption is not valid, especially in the case that sufficient and powerful error control method cannot be implemented over the feedback channel. As such, the study of the impact of imperfect feedback channels is very important. For instance, in [25], [26], the impact of imperfect feedback channels on the performance was investigated and two feedback-detection strategies have been proposed to mitigate the performance degradation and to reduce the outage region due to feedback errors. In this paper, we take a different point of view from that of [25], [26] and show that receiver diversity can be utilized to compensate for feedback error with the adjustment of the combiner structure.

We first consider the effect of feedback error on the performance of the joint AMDC systems and study the usage of adaptive combining at the receiver to mitigate this effect. We assume that feedback error may induce that the adaptive modulation mode used for transmission may be different from the one selected by the receiver after adaptive combining. To accommodate for such scenarios, the transmitter needs to inform the receiver which mode it will be using before the actual data transmission. We propose to use diversity path adjustment at the receiver to mitigate the error performance degradation or explore additional power savings. Specifically, the receiver may combine more diversity paths, if possible, to compensate for the bit error rate (BER) degradation when the transmitter sends data with a higher modulation mode than the one selected by the receiver. On the other hand, the receiver may use less diversity paths to save the receiver processing power when the transmitter sends data with a lower modulation mode. Hence, the number of combined paths can be adaptively changed depending on the nature of feedback error. We investigate the impact of this compensation method by analyzing the average number of combined paths, the average spectral efficiency, and the average BER of the joint AMDC scheme proposed in [12] in the presence of feedback error with and without adaptive combining path adjustment. We show through selected numerical examples that the proposed compensation strategy can offer considerable error performance improvement with little loss in processing power and spectral efficiency in comparison with the no compensation case.

The remainder of this paper is organized as follows. In Section II, we present the channel and

system model as well as the mode of operation of the joint AMDC scheme under consideration. Section III explains our proposed path adjustment scheme for the feedback error compensation and suggests a method to map the modulation mode into the feedback channel symbols and how to quantify feedback error over fading channels. In Section IV, we analyze the performance of the proposed system in terms of the average number of combined paths, the average spectral efficiency, and the average BER in the presence of feedback error. Some selected numerical examples and related discussions are presented in Section V. Finally, Section VI provides some concluding remarks.

II. Channel and System Model

A. Signal and Channel Model

Basically, we adopt the same signal and channel model as in [12]. We assume that the joint AMDC scheme is implemented in a discrete-time fashion. More specifically, short guard periods are periodically inserted into the transmitted signal. During these guard periods, the receiver performs a series of operations, including path estimations and combined signal-to-noise ratio (SNR) comparisons with respect to the predetermined SNR threshold. After determining the most appropriate diversity combiner structure and adaptive modulation mode to be used during the subsequent data burst, the receiver sends back the adaptive modulation mode to the transmitter via reverse link before the guard period ends. Because of feedback channel imperfection, the modulation mode used for transmission may be different from the one selected by the receiver. We assume that the transmitter informs the receiver about the actual transmitting mode before transmission.

We assume both flat fading with multiple antennas and selective fading with RAKE receiver. With this assumption, different diversity paths correspond to different resolvable paths. We also adopt a block fading model where the fading coefficients are assumed to be constant through the data burst period. As such, all the diversity paths experience almost the same fading conditions and maintain therefore the same SNR during the data burst and its preceding guard period.

Moreover, the fading conditions are assumed to follow the Rayleigh model and to be independent and identically distributed (i.i.d.) across the diversity paths and between different guard periods and data bursts. Hence, if we let γ_i denote the instantaneous received SNR of the ith path, $i = 1, 2, \cdots, L$, where L is the number of available diversity paths at the receiver, then the faded SNR, γ_i, follows the same exponential distribution, with common probability density function (PDF) and cumulative distribution function (CDF) given as [8, Eq. (6.5)]

$$f_{\gamma_i}(x) = \frac{1}{\overline{\gamma}} \exp\left(-\frac{x}{\overline{\gamma}}\right), \quad x \geq 0 \tag{1}$$

and

$$F_{\gamma_i}(x) = 1 - \exp\left(-\frac{x}{\overline{\gamma}}\right), \quad x \geq 0, \tag{2}$$

respectively, where $\overline{\gamma}$ is the common average faded SNR.

In what follows, it is assumed that the forward and feedback channels are independent so that we can ignore the correlation between two channels. This assumption is realizable if we consider frequency division duplex (FDD) where the frequency separation between uplink and downlink channels is much greater than the channel coherent bandwidth.

B. Joint Adaptive Modulation and Diversity Combining

We adopt the constant-power variable-rate uncoded M-ary quadrature amplitude modulation (M-QAM) scheme[1], where the modulation mode, M, is restricted to a power of 2, 2^n. Assume that the SNR range is divided into $N+1$ regions and each region is associated with a particular QAM signal constellation. The region boundaries, denoted by γ_{T_n}, are set to the SNR required to achieve the target BER, denoted by BER_0, using 2^n-QAM over an additive white Gaussian noise (AWGN) channel. It has been shown that the instantaneous BER of 2^n-QAM with two-dimentional Gray coding over an AWGN channel with SNR of γ can be well approximated by [3, Eq. (28)]

$$\text{BER}_n(\gamma) = \frac{1}{5} \exp\left(-\frac{3\gamma}{2(2^n - 1)}\right), \quad n = 1, 2, \cdots, N. \tag{3}$$

[1]Using the adaptively coded schemes in [2], [4], our results can be easily extended to coded systems

Therefore, the boundary thresholds can be calculated in terms of a target BER, BER_0, as

$$\gamma_{T_n} = \begin{cases} -\frac{2}{3}\ln(5\text{BER}_0)(2^n - 1), & n = 0, 1, \cdots, N; \\ \infty, & n = N + 1. \end{cases} \tag{4}$$

The receiver chooses the most suitable modulation mode, n, or constellation size, $M = 2^n$, based solely on the fading channel conditions. This is done by first examining the received SNR and then finding a proper region in which its estimated SNR falls. If the estimated SNR is in the nth region, the receiver informs via feedback path the corresponding modulation mode to the transmitter so that the constellation size of 2^n is used during the subsequent data burst.

Now we consider the joint AMDC schemes proposed in [12]. Specifically, we focus on the bandwidth-efficient and power-greedy AMDC scheme [12, Sec. V] since it has been shown to provide the better power efficiency than the bandwidth-efficient AMDC scheme while maintaining the same spectral efficiency as the bandwidth-efficient AMDC scheme. The basic principle behind the bandwidth-efficient and power-greedy AMDC scheme is to combine the smallest number of diversity paths such that the highest achievable modulation mode can be used while satisfying the instantaneous BER requirement. More specifically, during the guard period, the receiver estimates all L diversity paths and ranks them yielding the ordered SNRs, $\gamma_{1:L} > \gamma_{2:L} > \cdots > \gamma_{L:L}$, where $\gamma_{k:j}$ is the kth order statistics among j ones (see [18] for terminology). By using the MS-GSC scheme [20]–[22], the receiver first finds the highest modulation mode that can be used based on the current fading channel condition. Once the modulation mode is selected, then the receiver turns off as many of the weakest paths as possible such that the combined SNR of the remaining paths is large enough for the selected modulation mode to be used. If, in the worst case, the combined SNR of all L available paths is still below γ_{T_1}, the receiver may ask the transmitter to either transmit using the lowest modulation mode in violation of the target instantaneous BER requirement (option 1), or buffer the data and wait until the next guard period for more favorable channel conditions (option 2). The alternative but equivalent flowchart for the bandwidth-efficient and power-greedy AMDC scheme is illustrated in [11, Fig. 1].

III. Feedback Error and its Quantification

In this section, a detailed algorithm of the feedback error compensation for the bandwidth-efficient and power-greedy AMDC scheme is proposed. Then, we present as an example a modulation symbol labeling scheme for the feedback channel and show how to quantify feedback error over fading channels. Note that for the sake of clarity, we confine our discussion to option 2 in this section. By using a similar method, one may devise many alternative labeling schemes and quantify accordingly feedback error for both options 1 and 2.

A. Path Adjustment for Feedback Error Compensation

Assume that after performing a series of operations described in the previous section, the receiver decides to use the modulation mode $j\,(0 \leq j \leq N)$ with $l\,(0 \leq l \leq L)$ strongest paths. The receiver sends the index of this modulation mode, j, to the transmitter via the feedback channel but due to a possible feedback error the transmitter may end up using mode $n\,(0 \leq n \leq N)$ instead of j for transmission. We assume that the transmitter always informs the receiver about the actual transmitting mode[2], i.e., the receiver has the knowledge of n before the transmission occurs. We propose to use path adjustment for the case of feedback error. If $j > n$, for $n > 0$ the receiver reduces the combined paths by sequentially removing the weakest paths until either the combined SNR satisfies the new output threshold, γ_{T_n}, or the number of combined paths is 1. If $j < n$, then the receiver will combine all L paths in order to maximally improve the system performance since based on the mode of operation the AMDC scheme, the output SNR with L combined paths should still be between γ_{T_j} and $\gamma_{T_{j+1}}$ (i.e., $\gamma_{T_j} \leq \Gamma_{L:L} \leq \gamma_{T_{j+1}}$ where $\Gamma_{i:j}$ is the sum of the i largest SNRs among j ones, i.e., $\Gamma_{i:j} = \sum_{k=1}^{i} \gamma_{k:j}$). Finally, no path adjustment is necessary if $j = n$. Note that for option 2, no transmission occurs only when $j \geq n = 0$. The path adjustment algorithm for the bandwidth-efficient and power-greedy AMDC scheme with option 2 in the presence of feedback error is depicted in Fig. 1.

[2]In order to focus on the effect of feedback error, we assume that the actual mode information is protected by the strong code.

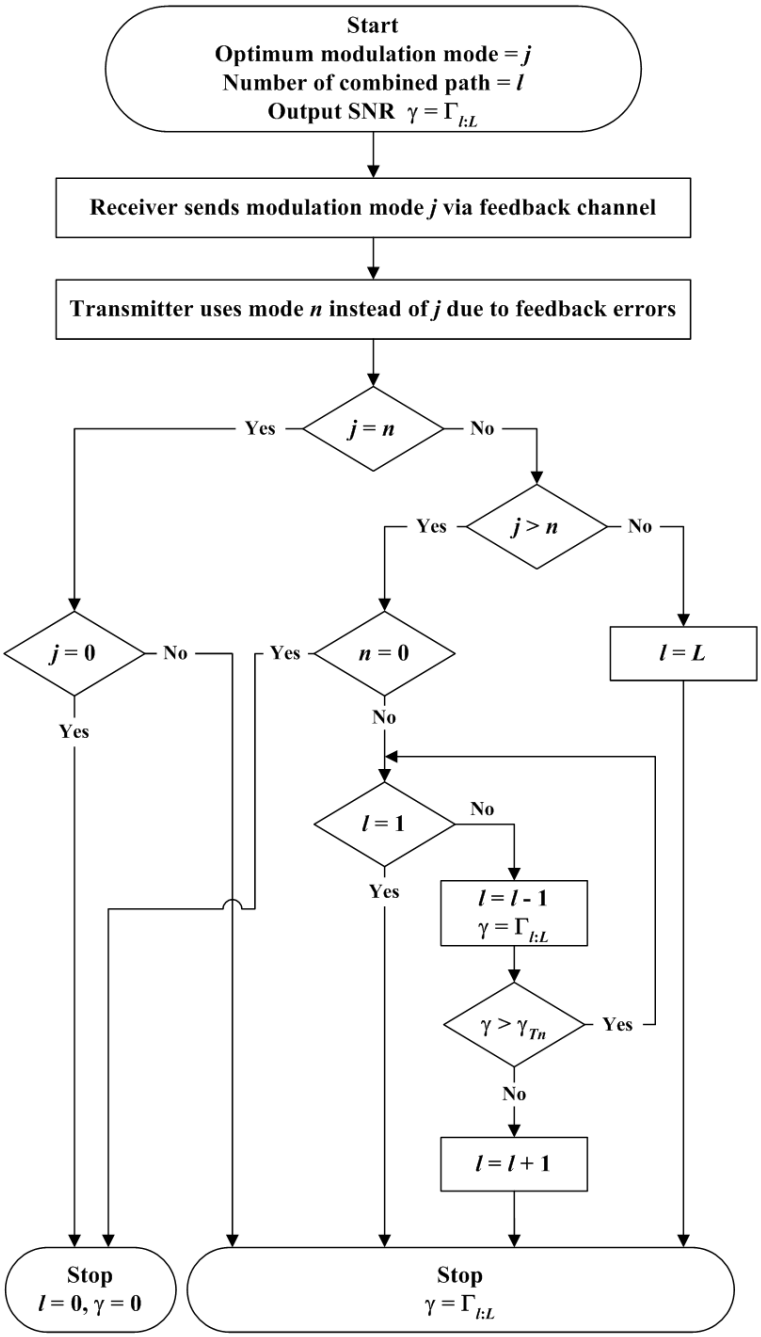

Fig. 1. Path adjustment algorithm for the bandwidth-efficient and power-greedy AMDC scheme with option 2.

B. Quantification of Feedback Error

To evaluate the effect of the feedback error and the compensation strategy introduced in the previous subsection, we need to determine the probability that the transmission mode n is used while mode j was selected by the receiver due to feedback error. We denote these mode transition probabilities by $q_{n,j}$ in the following. Note that these probabilities depend on the quality of the feedback channel and the signalling scheme used. In this work, we assume a phase shift keying (PSK) based signalling scheme over the feedback channel. More specifically, we use $N+1$ different PSK symbols to represent the total $N+1$ transmission modes. The receiver needs to transmit only one symbol during the guard period to indicate the selected mode.

If we assume that each transmission mode is sequentially mapped to each PSK symbol, then the decision region of the ith symbol representing the ith transmission mode will be the ith wedge-shaped area in the PSK signal space. Therefore, the mode transition probability, $q_{n,j}$, is equal to the average probability that the decision variable for the feedback channel detection falls erroneously in the nth wedge-shaped area instead of the jth wedge-shaped area. Since the transition probability, $q_{n,j}$, can be expressed as a function of the difference of mode indices, j and n, which can be calculated in a circular fashion as

$$a = \min\{|n-j|, N+1-|n-j|\}, \tag{5}$$

the instantaneous transition probability is equal to the probability that the decision variable falls in the wedge-shaped region between two different phase angles,

$$\theta_1 = \frac{(2a-1)\pi}{N+1} \text{ and } \theta_2 = \frac{(2a+1)\pi}{N+1},$$

when the symbol with phase zero was transmitted. It can be shown that this probability can be

calculated as [27, Eq. (17)]

$$\begin{aligned}\Psi(\gamma_s;\theta_1,\theta_2) = {} & Q(\sqrt{2\gamma_s}\sin\theta_1) - Q(\sqrt{2\gamma_s}\sin\theta_2) \\ & + Q\left(-\sqrt{2\gamma_s}\sin\theta_1, 0; \frac{\left(\sqrt{2\gamma_s}\sin\theta_2 - \cos(\theta_2-\theta_1)\sqrt{2\gamma_s}\sin\theta_1\right)\text{sgn}(\sqrt{2\gamma_s}\sin\theta_1)}{\sqrt{2\gamma_s\sin^2\theta_1 - 4\cos(\theta_2-\theta_1)\gamma_s\sin\theta_1\sin\theta_2 + 2\gamma_s\sin^2\theta_1}}\right) \\ & + Q\left(\sqrt{2\gamma_s}\sin\theta_2, 0; \frac{\left(\sqrt{2\gamma_s}\sin\theta_1 - \cos(\theta_2-\theta_2)\sqrt{2\gamma_s}\sin\theta_2\right)\text{sgn}(\sqrt{2\gamma_s}\sin\theta_2)}{\sqrt{2\gamma_s\sin^2\theta_1 - 4\cos(\theta_2-\theta_1)\gamma_s\sin\theta_1\sin\theta_2 + 2\gamma_s\sin^2\theta_1}}\right) \\ & - \Lambda(-2\gamma_s\sin\theta_1\sin\theta_2),\end{aligned} \tag{6}$$

where γ_s is the instantaneous symbol SNR of the feedback channel, $Q(\cdot)$ and $Q(\cdot,\cdot;\cdot)$ are the 1-D and 2-D Gaussian Q-functions, respectively, $\text{sgn}(x) = \begin{cases} 1, & x \geq 0; \\ -1, & x < 0, \end{cases}$ and $\Lambda(x) = \begin{cases} 0, & x \geq 0; \\ 1/2, & x < 0. \end{cases}$

Finally, noting that due to Rayleigh fading, the instantaneous SNR, γ_s, of the feedback channel is a random variable, we can obtain the mode transition probability, $q_{n,j}$, by averaging over its distribution as

$$q_{n,j} = \int_0^\infty \Psi\left(\gamma_s; \frac{(2a-1)\pi}{N+1}, \frac{(2a+1)\pi}{N+1}\right) f_{\gamma_s}(\gamma_s)d\gamma_s, \tag{7}$$

where $f_{\gamma_s}(\cdot)$ is the PDF of the faded SNR of the feedback channel, given in (1) but with average $\overline{\gamma}_s$. After substituting (1) and (6) with (5) into (7), the transition probability, $q_{n,j}$, can be shown to be a function of the average SNR, $\overline{\gamma}_s$, of the feedback channel. One can easily relate this average SNR with the average BER of $(N+1)$-PSK over Rayleigh fading channels, denoted by P_b. For example, when $N = 3$, we have $P_b = \frac{1}{2}\left(1 - \sqrt{\frac{\overline{\gamma}}{1+\overline{\gamma}}}\right)$ where $\overline{\gamma} = \overline{\gamma}_s/2$ [10, Eq. (8.104)]. In Table I, the transition probability, $q_{n,j}$, for this PSK-based sequential labeling scheme with option 2 is calculated as a function of the average BER, P_b, and the required average symbol SNR, $\overline{\gamma}_s$, of the feedback channel when $N = 3$.

Note that with this sequential labeling scheme, the symbol for the highest transmission mode is adjacent to the symbol for the lowest mode. One may think of other labeling schemes in which no adjacent symbols for the highest and lowest modes exist. In this case, because of the lower chance of transition between the highest and the lowest modulation indices, we can in general expect a higher spectral efficiency with more combined paths than the sequential labeling

TABLE I

TRANSITION PROBABILITY, $q_{n,j}$, WITH OPTION 2 OVER RAYLEIGH FADING CHANNELS FOR DIFFERENT AVERAGE BERS, P_b, WITH REQUIRED AVERAGE SNRS, $\overline{\gamma}_s$, OF THE FEEDBACK CHANNEL WHEN $N = 3$.

	$P_b = 10^{-1}$ $\overline{\gamma}_s = 5.51$ dB	$P_b = 10^{-2}$ $\overline{\gamma}_s = 16.86$ dB	$P_b = 10^{-3}$ $\overline{\gamma}_s = 26.98$ dB
$\lvert n-j\rvert = 0$	0.8218206	0.9818155	0.9981819
$\lvert n-j\rvert = 1, 3$	0.0781789	0.0081057	0.0008180
$\lvert n-j\rvert = 2$	0.0218214	0.0018491	0.0001820

scheme in the high SNR region and a lower spectral efficiency with less combined paths in the low SNR region. This difference will be increasing as feedback error increases.

IV. PERFORMANCE ANALYSIS IN THE PRESENCE OF FEEDBACK ERROR

In this section, we analyze the performance of the bandwidth-efficient and power-greedy AMDC scheme with feedback error over Rayleigh fading channels. More specifically, we obtain its average number of combined paths, average spectral efficiency, and average BER. In the following analysis, we assume that the mode transition probability, $q_{n,j}$, due to feedback error is calculated for both options 1 and 2 from the analysis in the previous section.

A. Average Number of Combined Paths

The average number of combined paths, $\overline{N}_c$, of the bandwidth-efficient and power-greedy AMDC scheme without feedback error compensation can be found in [12, Eq. (24)] as

$$\overline{N}_c = \begin{cases} \sum_{l=1}^{L} l \sum_{n=1}^{N} \Pr\left[\Gamma_{l-1:L} < \gamma_{T_n} < \Gamma_{l:L}, \Gamma_{L:L} < \gamma_{T_{n+1}}\right] + L \Pr\left[\Gamma_{L:L} < \gamma_{T_1}\right], & \text{for option 1;} \\ \sum_{l=1}^{L} l \sum_{n=1}^{N} \Pr\left[\Gamma_{l-1:L} < \gamma_{T_n} < \Gamma_{l:L}, \Gamma_{L:L} < \gamma_{T_{n+1}}\right], & \text{for option 2.} \end{cases} \tag{8}$$

With feedback error compensation, as mentioned in Section III-A, if $j > n$, the receiver will reduce the combined paths while all L paths are combined when $j < n$. Let $P_{l,n,j}$ denote the

probability that mode n is used with l combined paths while the true constellation size is j. Then, the average number of combined paths with feedback error is given for option 1 by

$$\overline{N}_c = \sum_{l=1}^{L} l \sum_{j=1}^{N} \sum_{n=1}^{j} q_{n,j}\, P_{l,n,j} + L\, q_{1,1}\, \Pr\left[\Gamma_{L:L} < \gamma_{T_1}\right] \tag{9}$$

$$+L \sum_{j=1}^{N-1} \sum_{n=j+1}^{N} q_{n,j} \times \begin{cases} \Pr\left[\Gamma_{L:L} < \gamma_{T_{j+1}}\right], & j = 1; \\ \Pr\left[\gamma_{T_j} < \Gamma_{L:L} < \gamma_{T_{j+1}}\right], & j > 1 \end{cases}$$

and for option 2 by

$$\overline{N}_c = \sum_{l=1}^{L} l \sum_{j=1}^{N} \sum_{n=1}^{j} q_{n,j}\, P_{l,n,j} + L \sum_{j=0}^{N-1} \sum_{n=j+1}^{N} q_{n,j}\, \Pr\left[\gamma_{T_j} < \Gamma_{L:L} < \gamma_{T_{j+1}}\right]. \tag{10}$$

Noting that $P_{l,n,j}$ is only valid when $n \leq j$, we can express $P_{l,n,j}$ for each case as

$$P_{l,n,j} = \begin{cases} \Pr\left[\Gamma_{l-1:L} < \gamma_{T_n} < \Gamma_{l:L}, \gamma_{T_j} < \Gamma_{L:L} < \gamma_{T_{j+1}}\right], & n \neq j < N; \\ \Pr\left[\Gamma_{l-1:L} < \gamma_{T_n} < \Gamma_{l:L}, \gamma_{T_N} < \Gamma_{L:L}\right], & n \neq j = N; \\ \Pr\left[\Gamma_{l-1:L} < \gamma_{T_n} < \Gamma_{l:L}, \Gamma_{L:L} < \gamma_{T_{n+1}}\right], & n = j < N; \\ \Pr\left[\Gamma_{l-1:L} < \gamma_{T_N} < \Gamma_{l:L}\right], & n = j = N. \end{cases} \tag{11}$$

All the probabilities in (11) can be obtained by using the results in [12]. For example,

$$\Pr\left[\Gamma_{l-1:L} < \gamma_{T_n} < \Gamma_{l:L}, \gamma_{T_j} < \Gamma_{L:L} < \gamma_{T_{j+1}}\right] \tag{12}$$

$$= \Pr\left[\Gamma_{l-1:L} < \gamma_{T_n} < \Gamma_{l:L}, \Gamma_{L:L} < \gamma_{T_{j+1}}\right] - \Pr\left[\Gamma_{l-1:L} < \gamma_{T_n} < \Gamma_{l:L}, \Gamma_{L:L} < \gamma_{T_j}\right].$$

Let y_l denote the sum of the $l-1$ largest ordered-path SNRs, i.e., $y_l = \Gamma_{l-1:L}$, and z_l denote the sum of the $L-l$ smallest ordered-path SNRs, i.e., $z_l = \Gamma_{L:L} - \Gamma_{l:L}$. Then, we can have the

general form of the probability, $\Pr\left[\Gamma_{l-1:L} < \alpha < \Gamma_{l:L}, \Gamma_{L:L} < \beta\right]$, in (12) for $\alpha < \beta$ as[3]

$$\begin{aligned}
&\Pr\left[\Gamma_{l-1:L} < \alpha < \Gamma_{l:L}, \Gamma_{L:L} < \beta\right] \qquad (13)\\
&= \Pr\left[y_l < \alpha < y_l + \gamma_{l:L},\ y_l + \gamma_{l:L} + z_l < \beta\right]\\
&= \begin{cases}
\begin{cases}
\int_{\alpha}^{\beta}\int_{0}^{\beta-\gamma} f_{\gamma_{1:L},z_1}(\gamma,z)dzd\gamma, & L\alpha \geq \beta;\\
\int_{\alpha}^{\beta/L}\int_{0}^{(L-1)\gamma} f_{\gamma_{1:L},z_1}(\gamma,z)dzd\gamma & \\
\quad + \int_{\beta/L}^{\beta}\int_{0}^{\beta-\gamma} f_{\gamma_{1:L},z_1}(\gamma,z)dzd\gamma, & L\alpha < \beta,
\end{cases} & l = 1;\\
\begin{cases}
\int_{(l-1)\alpha/l}^{\alpha}\int_{\alpha-y}^{y/(l-1)}\int_{0}^{\beta-y-\gamma} f_{y_l,\gamma_{l:L},z_l}(y,\gamma,z)dzd\gamma dy, & l\alpha \leq (l-1)\beta;\\
\int_{(l-1)\alpha/l}^{(l-1)\beta/l}\int_{\alpha-y}^{y/(l-1)}\int_{0}^{\beta-y-\gamma} f_{y_l,\gamma_{l:L},z_l}(y,\gamma,z)dzd\gamma dy & \\
\quad + \int_{(l-1)\beta/l}^{\alpha}\int_{\alpha-y}^{\beta-y}\int_{0}^{\beta-y-\gamma} f_{y_l,\gamma_{l:L},z_l}(y,\gamma,z)dzd\gamma dy, & l\alpha > (l-1)\beta,
\end{cases} & 1 < l < L;\\
\begin{cases}
\int_{(L-1)\alpha/L}^{\alpha}\int_{\alpha-y}^{y/(L-1)} f_{y_L,\gamma_{L:L}}(y,\gamma)d\gamma dy, & L\alpha \leq (L-1)\beta;\\
\int_{(L-1)\beta/L}^{(L-1)\beta/L}\int_{\alpha-y}^{y/(L-1)} f_{y_L,\gamma_{L:L}}(y,\gamma)d\gamma dy & \\
\quad + \int_{(L-1)\beta/L}^{\alpha}\int_{\alpha-y}^{\beta-y} f_{y_L,\gamma_{L:L}}(y,\gamma)d\gamma dy, & L\alpha > (L-1)\beta,
\end{cases} & l = L.
\end{cases}
\end{aligned}$$

It has been shown that the joint PDF, $f_{y_l,\gamma_{l:L},z_l}(y,\gamma,z)$, in (13) over i.i.d. Rayleigh fading channels is given in [12, Eq. (21)]. The other joint PDFs, $f_{\gamma_{1:L},z_1}(\gamma,z)$ and $f_{y_L,\gamma_{L:L}}(y,\gamma)$, in (13) can be obtained as marginal PDFs of [12, Eq. (21)]. After successive substitutions from (13) to (9) and (10), we can obtain the average number of combined paths, $\overline{N}_c$, of the bandwidth-efficient and power-greedy AMDC scheme with feedback error compensation.

B. Average Spectral Efficiency

In case of no feedback error, the average spectral efficiency, η, of the adaptive system can be calculated as [3, Eq. (33)]

$$\eta = \sum_{n=1}^{N} n\,\pi_n, \qquad (14)$$

[3]Note that Eq. (13) is the complement version of [12, Eq. (27)].

where π_n is the probability that nth modulation mode is used which can be expressed for the bandwidth-efficient and power-greedy AMDC scheme as [12]

$$\pi_n = \begin{cases} \begin{cases} F^{\text{MSC}(\gamma_{T_N})}(\gamma_{T_{n+1}}) - F^{\text{MSC}(\gamma_{T_N})}(\gamma_{T_n}), & n > 1; \\ F^{\text{MSC}(\gamma_{T_N})}(\gamma_{T_2}), & n = 1, \end{cases} & \text{for option 1;} \\ F^{\text{MSC}(\gamma_{T_N})}(\gamma_{T_{n+1}}) - F^{\text{MSC}(\gamma_{T_N})}(\gamma_{T_n}), & \text{for option 2,} \end{cases} \tag{15}$$

where $F^{\text{MSC}(\gamma_{T_N})}(\cdot)$ denotes the CDF of the combined SNR with L-branch MS-GSC and using γ_{T_N} as an output threshold and which is given for i.i.d. Rayleigh fading channels in [22, Eq. (20)]. With feedback error, we can obtain the average spectral efficiency for both options as

$$\eta = \sum_{n=1}^{N} \sum_{\substack{j=0 \\ \text{for option 2} \\ j=1 \\ \text{for option 1}}}^{N} n\, q_{n,j}\, \pi_j, \tag{16}$$

where $q_{n,j}$ is the mode transition probability due to feedback error and π_j is given above in (15).

C. Average Error Rate

The average BER for the adaptive modulation system can be calculated as [3, Eq. (35)]

$$\text{BER} = \frac{1}{\eta} \sum_{n=1}^{N} n \cdot \overline{\text{BER}}_n, \tag{17}$$

where $\overline{\text{BER}}_n$ is the average error rate when constellation size n is used for transmission. When there is feedback error and the system does not adjust the number of combined paths, $\overline{\text{BER}}_n$ can be calculated as

$$\overline{\text{BER}}_n = \begin{cases} q_{n,1} \int_0^{\gamma_{T_2}} \text{BER}_n(x) f_\gamma(x) dx + \sum\limits_{j=2}^{N} q_{n,j} \int_{\gamma_{T_j}}^{\gamma_{T_{j+1}}} \text{BER}_n(x) f_\gamma(x) dx, & \text{for option 1;} \\ \sum\limits_{j=0}^{N} q_{n,j} \int_{\gamma_{T_j}}^{\gamma_{T_{j+1}}} \text{BER}_n(x) f_\gamma(x) dx, & \text{for option 2,} \end{cases} \tag{18}$$

where $f_\gamma(\cdot)$ is the PDF of the output SNR which has been obtained in [12, Eq. (23)].

If the system adjusts the combiner structure for the case of feedback error, the calculation of $\overline{\text{BER}}_n$ is more complicated since in this case the PDF of the output SNR is varying with combiner adjustment. Specifically, we consider the case of $j < n$ and $j \geq n$ separately. Let

$f_\gamma^-(x)$ denote the PDF of the output SNR after adjustment for $j < n$ case and $f_\gamma^+(x)$ for $j \geq n$ case. Then, $\overline{\text{BER}}_n$ for option 2 can be written as

$$\overline{\text{BER}}_n = \sum_{j=0}^{n-1} q_{n,j} \int_{\gamma_{T_j}}^{\gamma_{T_{j+1}}} \text{BER}_n(x) f_\gamma^-(x) dx + \sum_{j=n}^{N} q_{n,j} \int_{\gamma_{T_n}}^{\gamma_{T_{n+1}}} \text{BER}_n(x) f_\gamma^+(x) d\gamma. \tag{19}$$

Noting that the receiver combines all L paths when the actual mode n is greater than the feedback mode j, the PDF, $f_\gamma^-(x)$, is simply the PDF of the L/L-GSC output SNR [10, Eq. (9.433)]. On the other hand, when $j \geq n$, the receiver will combine less paths as long as the output SNR is greater than γ_{T_n}. Therefore, the PDF of the output SNR, $f_\gamma^+(x)$, over the range of $[\gamma_{T_n}, \gamma_{T_{n+1}})$ can be determined as

$$\begin{aligned} f_\gamma^+(x) = \frac{d}{dx}\Bigg(& \Pr\left[\gamma_{T_n} < \Gamma_{1:L} < x, \gamma_{T_j} < \Gamma_{L:L} < \gamma_{T_{j+1}}\right] \\ & + \sum_{l=2}^{L} \Pr\left[\Gamma_{l-1:L} < \gamma_{T_n} < \Gamma_{l:L} < x, \gamma_{T_j} < \Gamma_{L:L} < \gamma_{T_{j+1}}\right] \Bigg). \end{aligned} \tag{20}$$

By using the results in [12], we can calculate each term in (20) as

$$\begin{aligned} & \frac{d}{dx} \Pr\left[\gamma_{T_n} < \Gamma_{1:L} < x, \gamma_{T_j} < \Gamma_{L:L} < \gamma_{T_{j+1}}\right] \\ & = \begin{cases} \int_0^{\gamma_{T_{j+1}} - \gamma_{T_j}} f_{\gamma_{1:L}, z_1}(x, z) dz, & n \neq j < N; \\ f_{\gamma_{1:L}}(x) - \int_0^{\gamma_{T_N} - x} f_{\gamma_{1:L}, z_1}(x, z) dz, & n \neq j = N; \\ \int_0^{\gamma_{T_{n+1}} - x} f_{\gamma_{1:L}, z_1}(x, z) dz, & n = j < N; \\ f_{\gamma_{1:L}}(x), & n = j = N, \end{cases} \end{aligned} \tag{21}$$

$$\begin{aligned} & \frac{d}{dx} \Pr\left[\Gamma_{l-1:L} < \gamma_{T_n} < \Gamma_{l:L} < x, \gamma_{T_j} < \Gamma_{L:L} < \gamma_{T_{j+1}}\right] \\ & = \begin{cases} \int_{\frac{l-1}{l}x}^{\gamma_{T_n}} \int_0^{\gamma_{T_{j+1}} - \gamma_{T_j}} f_{y_l, \gamma_{l:L}, z_l}(y, x-y, z) dz dy \left(\mathcal{U}(x - \gamma_{T_n}) - \mathcal{U}(x - \frac{l}{l-1}\gamma_{T_n})\right), & n \neq j < N; \\ \int_{\frac{l-1}{l}x}^{\gamma_{T_n}} f_{y_l, \gamma_{l:L}}(y, x-y) dy \left(\mathcal{U}(x - \gamma_{T_n}) - \mathcal{U}(x - \frac{l}{l-1}\gamma_{T_n})\right) & \\ \quad - \int_{\frac{l-1}{l}x}^{\gamma_{T_n}} \int_0^{\gamma_{T_N} - x} f_{y_l, \gamma_{l:L}, z_l}(y, x-y, z) dz dy \left(\mathcal{U}(x - \gamma_{T_n}) - \mathcal{U}(x - \frac{l}{l-1}\gamma_{T_n})\right), & n \neq j = N; \\ \int_{\frac{l-1}{l}x}^{\gamma_{T_n}} \int_0^{\gamma_{T_{n+1}} - x} f_{y_l, \gamma_{l:L}, z_l}(y, x-y, z) dz dy \left(\mathcal{U}(x - \gamma_{T_n}) - \mathcal{U}(x - \frac{l}{l-1}\gamma_{T_n})\right), & n = j < N; \\ \int_{\frac{l-1}{l}x}^{\gamma_{T_N}} f_{y_l, \gamma_{l:L}}(y, x-y) dy \left(\mathcal{U}(x - \gamma_{T_N}) - \mathcal{U}(x - \frac{l}{l-1}\gamma_{T_N})\right), & n = j = N, \end{cases} \end{aligned} \tag{22}$$

and

$$\frac{d}{dx}\Pr\left[\Gamma_{L-1:L} < \gamma_{T_n} < \Gamma_{L:L} < x, \gamma_{T_j} < \Gamma_{L:L} < \gamma_{T_{j+1}}\right] \tag{23}$$
$$= \begin{cases} 0, & n \neq j; \\ \int_{\frac{L-1}{L}x}^{\gamma_{T_n}} f_{y_L,\gamma_{L:L}}(y, x-y)dy \left(\mathcal{U}(x-\gamma_{T_n}) - \mathcal{U}(x-\frac{L}{L-1}\gamma_{T_n})\right), & n = j, \end{cases}$$

where $\mathcal{U}(\cdot)$ is the unit step function. Finally, substituting (21), (22), and (23) into (20), then (20) into (19), and finally (19) into (17) leads to the desired average BER of the bandwidth-efficient and power-greedy AMDC scheme for option 2 with feedback error over Rayleigh fading channels. The average BER for option 1 can be similarly obtained.

V. Numerical Examples

In this section, we illustrate the analytical results derived in the previous section with some selected numerical examples. Note that although all numerical evaluations obtained from the analytical results derived in this paper have been also compared by Monte Carlo simulations of the system under consideration in order to justify our approach, for the better visual quality we plot the simulation results only for $P_b = 10^{-1}$ in all figures.

Keep in mind that only when there exists feedback error, the number of combined paths is changed by the proposed path adjustment algorithm in order to accommodate the erroneously selected modulation mode, n. Hence, the average spectral efficiency is just dependent on feedback error and is not affected by path adjustment. In Fig. 2, we present the average number of combined paths of the bandwidth-efficient and power-greedy AMDC scheme with option 2 for different average BERs, P_b, of the feedback channel as a function of the average SNR per path, $\overline{\gamma}$, when $L = 5, N = 3$, and $\text{BER}_0 = 10^{-3}$. In this figure and what follows, we use the transition probability, $q_{n,j}$, in Table I obtained from the labeling scheme presented in Section III-B. From this figure, we can observe that if the average BER of the feedback channel is relatively small, i.e., $P_b = 10^{-2}$ and 10^{-3}, the average number of combined paths is almost the same as that in the case of no feedback error, which means in this case feedback error does not significantly

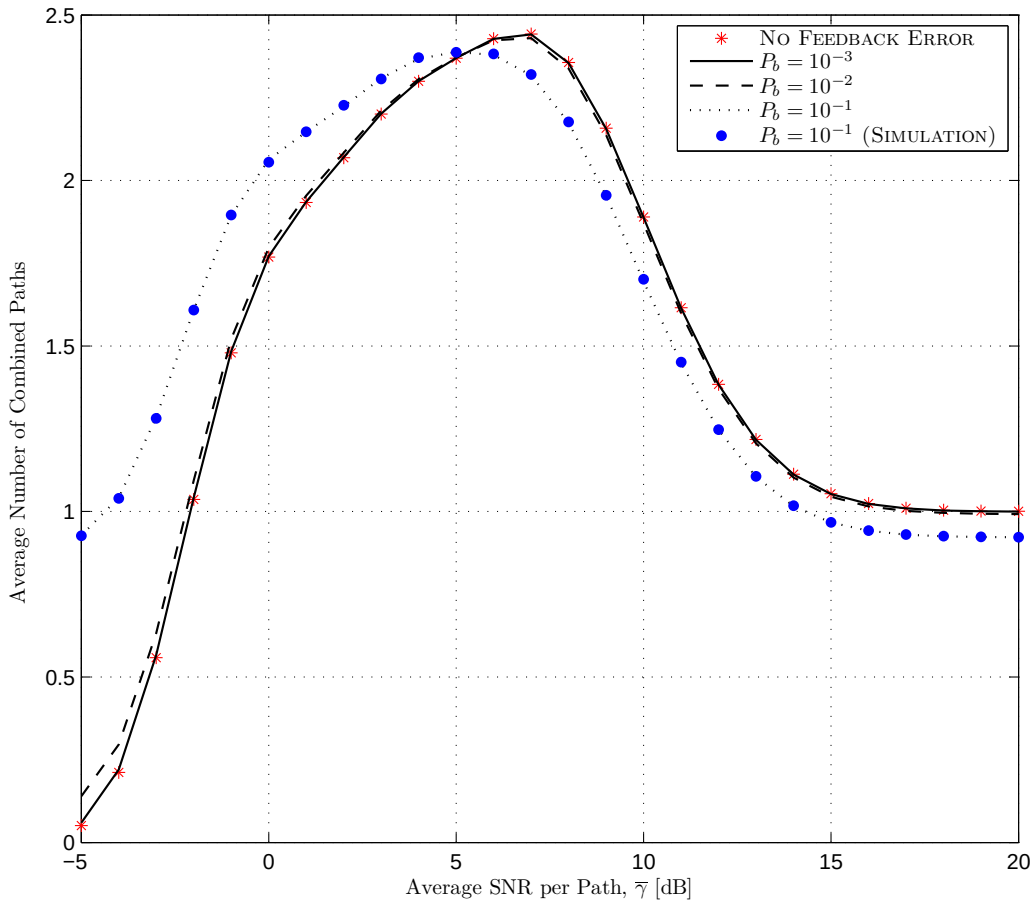

Fig. 2. Average number of combined paths of the bandwidth-efficient and power-greedy AMDC scheme with option 2 for different average BERs, P_b, of the feedback channel as a function of the average SNR per path, $\overline{\gamma}$, when $L = 5, N = 3$, and $\text{BER}_0 = 10^{-3}$.

affect the performance measure. On the other hand, when $P_b = 10^{-1}$, we can see that the system requires more paths over the low SNR region and less paths over the high SNR region. Note that as the average BER of the feedback channel is increasing, the possibility of path adjustment is also increasing because of the high chance of having different values between n and j. In this case, for the low SNR region, the receiver has to combine more paths in order to satisfy the actual boundary threshold, γ_{T_n}, which is possibly larger than the true threshold, γ_{T_j}, while

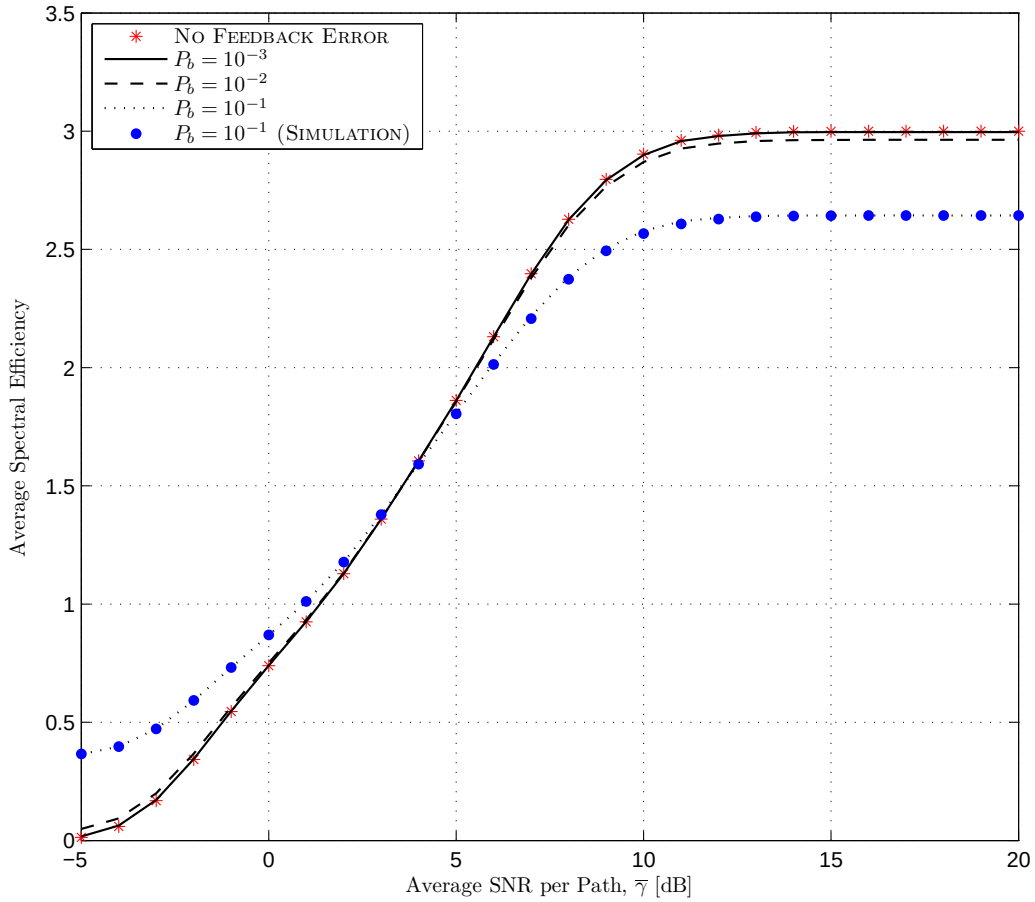

Fig. 3. Average spectral efficiency of the bandwidth-efficient and power-greedy AMDC scheme with option 2 for different average BERs, P_b, of the feedback channel as a function of the average SNR per path, $\overline{\gamma}$, when $L = 5$, $N = 3$, and $\text{BER}_0 = 10^{-3}$.

for the high SNR region, less paths are required to meet γ_{T_n} which is possibly smaller than γ_{T_j}. This observation can be verified and supported by Fig. 3 which shows the average spectral efficiency with the same parameters used in Fig. 2. While, with $P_b = 10^{-2}$ and 10^{-3}, giving almost the same value as that in the case of no feedback error, the average spectral efficiency with $P_b = 10^{-1}$ is larger over the low SNR region and smaller over the high SNR region than that without feedback error. Note that if the larger modulation mode ($N > 3$) is used, the difference in the average spectral efficiency between the cases of feedback error and no feedback error will

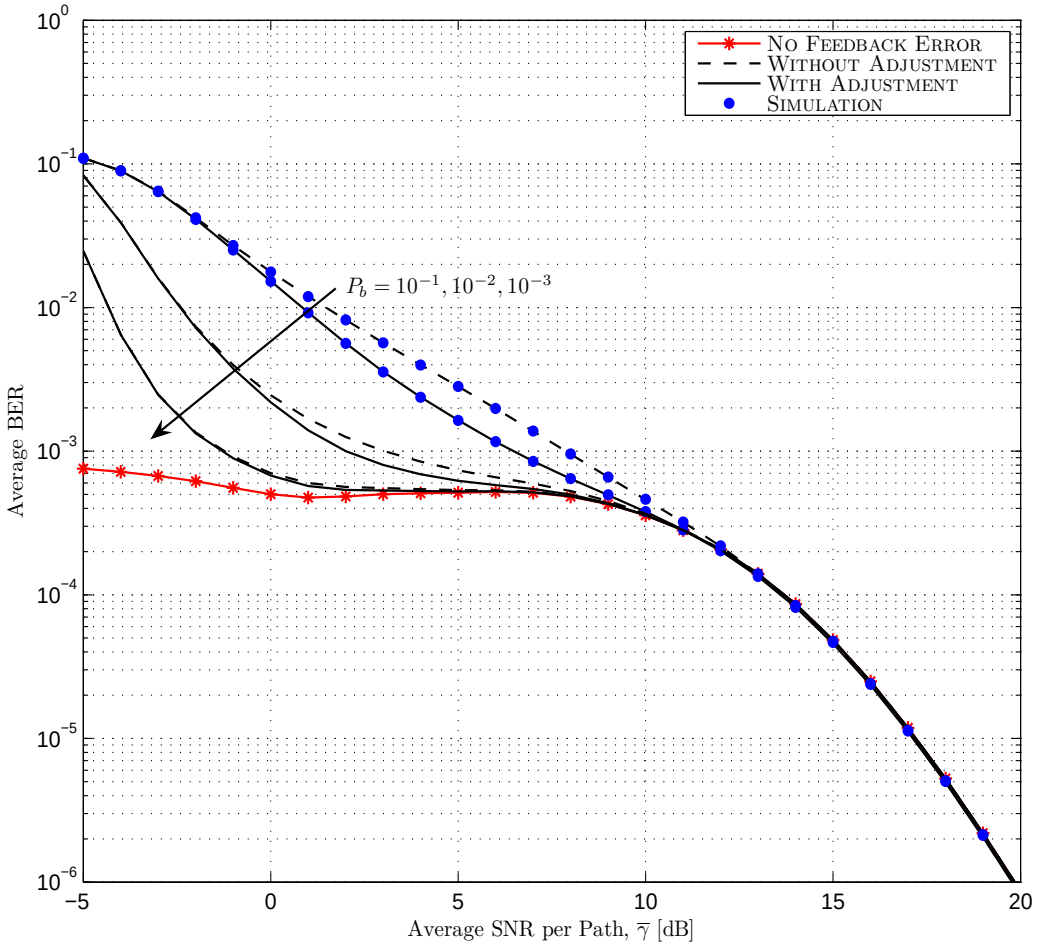

Fig. 4. Average BER of the bandwidth-efficient and power-greedy AMDC scheme with option 2 for different average BERs, P_b, of the feedback channel as a function of the average SNR per path, $\overline{\gamma}$, when $L = 5, N = 3$, and $\text{BER}_0 = 10^{-3}$.

be more distinct.

Finally, we examine the BER performance of the bandwidth-efficient and power-greedy AMDC scheme with option 2 in Fig. 4 under the same parameters used in the previous figures. This figure shows that feedback error considerably degrades the BER performance especially for the low SNR region. Now let us consider how path adjustment can compensate the performance loss due to feedback error. Fig. 4 shows that the gain obtained from path adjustment over medium

SNR range is the major benefit. For example, to meet a target $\text{BER}_0 = 10^{-3}$, with the feedback error $P_b = 10^{-1}$, the scheme without path adjustment requires 7.9 dB while the scheme with path adjustment only needs 6.5 dB (i.e., path adjustment yields 1.4 dB gains). When the feedback error $P_b = 10^{-2}$, about 1 dB SNR gain can be obtained from path adjustment. Also note that from Figs. 2 and 3, it is shown that in the middle range of SNR (i.e., between 5 and 10 dB), the bandwidth-efficient and power-greedy AMDC scheme with path adjustment in the presence of feedback error uses actually in average less combined paths and suffers a small loss in spectral efficiency in comparison with the perfect feedback case.

VI. Conclusions

In this paper, we studied the joint AMDC scheme for high spectral and power efficient wireless systems, taking into account imperfect feedback channel conditions. More specifically, it is assumed that the modulation mode the transmitter receives from the receiver can be perturbed by some feedback errors that can result in the usage of the wrong transmission mode between the transmitter and the receiver. In order to mitigate the performance impediment, the receiver adjusts its diversity combining structure according to the nature of feedback error. Through the analysis of this scheme, we have shown that our proposed path adjustment method can reduce the probability of error degradation while maintaining almost the same processing power and spectral efficiency in comparison with the scheme without path adjustment if the error probability of the feedback channel is not very high.

References

[1] A. J. Goldsmith and S. G. Chua, "Variable-rate variable-power M-QAM for fading channels," *IEEE Trans. Commun.*, vol. 45, no. 10, pp. 1218–1230, Oct. 1997.

[2] ——, "Adaptive coded modulation for fading channels," *IEEE Trans. Commun.*, vol. 46, no. 5, pp. 595–602, May 1998.

[3] M.-S. Alouini and A. J. Goldsmith, "Adaptive modulation over Nakagami fading channels," *Kluwer J. Wireless Commun.*, vol. 13, no. 1, pp. 119–143, May 2000.

[4] K. J. Hole, H. Holm, and G. E. Øien, "Adaptive multidimentional coded over flat fading channels," *IEEE J. Select. Areas Commun.*, vol. 18, no. 7, pp. 1153–1158, July 2000.

[5] N. C. Beaulieu, "Introduction to "linear diversity combining techniques"," *Proc. IEEE*, vol. 91, no. 2, pp. 328–356, Feb. 2003.

[6] W. C. Jakes, *Microwave Mobile Communications*, 2nd ed. Piscataway, NJ: IEEE Press, 1994.

[7] J. G. Proakis, *Digital Communications*, 3rd ed. New York, NY: McGraw-Hill, 1995.

[8] G. L. Stüber, *Principles of Mobile Communication*, 2nd ed. Norwell, MA: Kluwer Academic Publishers, 2001.

[9] T. S. Rappaport, *Wireless Communications : Principles and Practice*, 2nd ed. Upper Saddle River, NJ: Prentice Hall, 2002.

[10] M. K. Simon and M.-S. Alouini, *Digital Communication over Fading Channels*, 2nd ed. New York, NY: John Wiley & Sons, 2005.

[11] N. Belhaj, N. Hamdi, M.-S. Alouini, and A. Bouallegue, "Adaptive modulation and combining for bandwidth and power efficient communication over fading channels," *Wirel. Commun. Mob. Comput.*, vol. 7, pp. 513–529, 2007.

[12] H.-C. Yang, N. Belhaj, and M.-S. Alouini, "Performance analysis of joint adaptive modulation and diversity combining over fading channels," *IEEE Trans. Commun.*, vol. 55, no. 3, pp. 520–528, Mar. 2007.

[13] Y.-C. Ko, H.-C. Yang, S.-S. Eom, and M.-S. Alouini, "Adaptive modulation with diversity combining based on output-threshold MRC," *IEEE Trans. Wireless Commun.*, vol. 6, no. 10, pp. 3728–3737, Oct. 2007.

[14] M.-S. Alouini and A. J. Goldsmith, "Capacity of Rayleigh fading channels under different adaptive transmission and diversity-combining techniques," *IEEE Trans. Veh. Technol.*, vol. 48, no. 4, pp. 1165–1181, July 1999.

[15] R. K. Mallik, M. Z. Win, J. W. Shao, M.-S. Alouini, and A. J. Goldsmith, "Channel capacity of adaptive transmission with maximal ratio combining in correlated Rayleigh fading," *IEEE Trans. Wireless Commun.*, vol. 3, no. 4, pp. 1124–1133, July 2004.

[16] T. Eng, N. Kong, and L. B. Milstein, "Comparison of diversity combining techniques for Rayleigh-fading channels," *IEEE Trans. Commun.*, vol. 44, no. 9, pp. 1117–1129, Sept. 1996.

[17] M. Z. Win and J. H. Winters, "Analysis of hybrid selection/maximal-ratio combining in Rayleigh fading," *IEEE Trans. Commun.*, vol. 47, no. 12, pp. 1773–1776, Dec. 1999.

[18] M.-S. Alouini and M. K. Simon, "An MGF-based performance analysis of generalized selection combining over Rayleigh fading channels," *IEEE Trans. Commun.*, vol. 48, no. 3, pp. 401–415, Mar. 2000.

[19] Y. Ma and C. C. Chai, "Unified error probability analysis for generalized selection combining in Nakagami fading channels," *IEEE J. Select. Areas Commun.*, vol. 18, no. 11, pp. 2198–2210, Nov. 2000.

[20] S. W. Kim, D. S. Ha, and J. H. Reed, "Minimum selection GSC and adaptive low-power RAKE combining scheme," in *Proc. IEEE Int. Symp. on Circuit and Systems (ISCAS'03)*, Bangkok, Thailand, May 2003.

[21] R. K. Mallik, P. Gupta, and Q. T. Zhang, "Minimum selection GSC in independent Rayleigh fading," *IEEE Trans. Veh. Technol.*, vol. 54, no. 3, pp. 1013–1021, May 2005.

[22] H.-C. Yang, "New results on ordered statistics and analysis of minimum-selection generalized selection combining (GSC)," *IEEE Trans. Wireless Commun.*, vol. 5, no. 7, pp. 1876–1885, July 2006.

[23] M.-S. Alouini and H.-C. Yang, "Minimum estimation and combining generalized selection combining (MEC-GSC)," in *Proc. IEEE Int. Symp. on Information Theory (ISIT'05)*, Adelaide, Australia, Sept. 2005.

[24] H.-C. Yang and M.-S. Alouini, "MRC and GSC diversity combining with an output theshold," *IEEE Trans. Veh. Technol.*, vol. 54, no. 3, pp. 1081–1090, May 2005.

[25] A. E. Ekpenyong and Y.-F. Huang, "Feedback-detection strategies for adaptive modulation systems," *IEEE Trans. Commun.*, vol. 54, no. 10, pp. 1735–1740, Oct. 2006.

[26] ——, "Feedback constraints for adaptive transmission," *IEEE Signal Processing Mag.*, pp. 69–78, May 2007.

[27] S. Park and D. Yoon, "An alternative expression for the symbol-error probability of MPSK in the presence of I/Q unbalance," *IEEE Trans. Commun.*, vol. 52, no. 12, pp. 2079–2081, Dec. 2004.